Low frequency electromagnetic radiation from sprite streamers

Jianqi Qin,[1] Sebastien Celestin,[1] and Victor P. Pasko[1]

Received 23 September 2012; revised 17 October 2012; accepted 17 October 2012; published 27 November 2012.

[1] Sprites are mesospheric discharges that carry significant electrical currents and produce electromagnetic radiation observed typically in the extremely low (ELF) to ultra low (ULF) frequency bands. In this letter, we present the first theoretical estimates of the electromagnetic radiation produced by individual sprite streamers using simulation results from a plasma fluid model. It is demonstrated that the spectral content of the radiation produced by sprite streamers is a function of the air density N and the lightning-induced quasi-static ambient electric field E in the regions of space where the sprite streamers are propagating. We demonstrate that the exponential growth of the current in sprite streamers at 75 km would be preferentially associated with electromagnetic radiation in the frequency range from 0 and up to ~3 kHz, whereas the growth of the streamer current at 40 km could produce radiation with frequencies up to ~300 kHz, consistently with the scaling of atmospheric air density. We further conjecture that the periodic branching of streamers may lead to a radiation spectrum enhancement in the very low (VLF) to low frequency (LF) range. **Citation:** Qin, J., S. Celestin, and V. P. Pasko (2012), Low frequency electromagnetic radiation from sprite streamers, *Geophys. Res. Lett.*, *39*, L22803, doi:10.1029/2012GL053991.

1. Introduction

[2] Simultaneous observations of sprite-associated Extremely Low Frequency (ELF) radio atmospherics and sprite luminosity demonstrate that significant electrical current is flowing in the body of sprites, which produces detectable ELF electromagnetic (EM) power at levels comparable to that produced by the sprite-causative lightning discharge [*Cummer et al.*, 1998; *Cummer*, 2003], with the source locations of the ELF radiation being further confirmed to be in the mesosphere [*Fullekrug et al.*, 2001]. Recently, Low-Frequency (LF) radio observations of sprite-producing lightning discharges have shown the existence of consecutive broadband pulses exhibiting EM radiation that spans from ~50 to 350 kHz, and occurring also coincidentally with the sprite luminosity [*Fullekrug et al.*, 2010]. It has been suggested by *Fullekrug et al.* [2010, 2011] that this LF radiation may stem from non-luminous relativistic electron beams occurred at ~22–72 km altitudes above thunderstorms. The purpose of the present study is to estimate the characteristic frequencies of the EM radiation produced by individual sprite streamers using a streamer model. We demonstrate that sprite streamers at low altitude (~40 km) can produce radiation up to the LF range (30–300 kHz) because the characteristic timescale of the current variation in sprite streamers is inversely proportional to the air density.

2. Model Formulation

[3] In order to calculate the electric currents flowing in the body of sprite streamers, a two-dimensional cylindrically symmetric (r, z dependent) plasma fluid model developed by J. Qin et al. (Dependence of positive and negative sprite morphology on lightning characteristics and upper atmospheric ambient conditions, submitted to *Journal of Geophysical Research*, 2012) is used to simulate the dynamics of sprite streamers. In this model, the chemical reactions accounted for include the electron impact ionization of N_2 and O_2, the electron dissociative attachment to O_2, and the electron detachment process $O^- + N_2 \rightarrow e + N_2O$ [*Qin et al.*, 2012, equations (1)–(4)]. Photoionization processes are included using the three-group SP_3 model developed by *Bourdon et al.* [2007]. The motion of charged species is simulated by solving the drift-diffusion equations for electrons and ions coupled with the Poisson's equation [*Qin et al.*, 2012, equations (5)–(9)]. The transport equations for charged species are solved using a flux-corrected transport technique that combines an eighth-order scheme for the high-order fluxes and a donor cell scheme for the low-order fluxes.

[4] Sprite streamers are primarily vertical filamentary plasma discharges that have characteristic radii ~100 m at ~75 km [*Stenbaek-Nielsen and McHarg*, 2008], and become smaller at lower altitudes (e.g., ~1 m at 40 km) according to the similarity laws [*Pasko et al.*, 1998; *Liu and Pasko*, 2004]. In order to calculate their far field radiation, sprite streamers can be considered as vertical antennas with current variation at any locations $I(z, t)$ calculated by the plasma fluid model. This assumption is justified by our results showing that the radius of the streamer cross-section is at least three orders of magnitude smaller than the wavelength of any radiation under consideration. The analytical time-domain solution for the azimuthal magnetic component of the EM field from a finite antenna of length H (see Figure 1) is given by *Uman et al.* [1975]:

$$B_\phi(t) = \frac{\mu_0}{4\pi}\int_0^H \frac{\sin\theta}{R^2} i(z, t - R/c)dz + \frac{\mu_0}{4\pi}\int_0^H \frac{\sin\theta}{cR}\frac{\partial i(z, t - R/c)}{\partial t}dz \quad (1)$$

where i is the current flowing in the antenna, θ is the polar angle of the receiver with respect to the source location, R is the distance from the antenna to the receiver (see Figure 1), μ_0 and c are, respectively, the permeability and speed of

[1]Communications and Space Sciences Laboratory, Department of Electrical Engineering, Pennsylvania State University, University Park, Pennsylvania, USA.

Corresponding author: J. Qin, Communications and Space Sciences Laboratory, Department of Electrical Engineering, Pennsylvania State University, 227 EE East, University Park, PA 16802-2706, USA. (jianqiqin@psu.edu)

0094-8276/12/2012GL053991

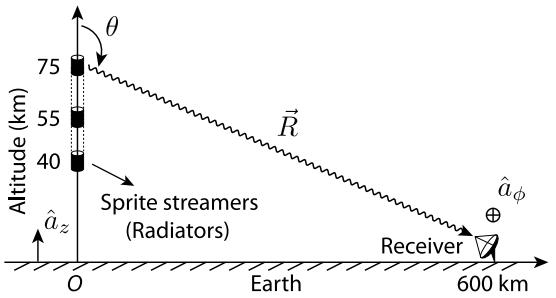

Figure 1. Geometry of the EM radiation from a sprite.

light in vacuum. Note that although it is included in our calculations, the contribution from the first term in equation (1) is negligible for the far field radiation. Fourier transform is then applied to calculate the spectrum of the sprite radiation using $B_\phi(t)$, which is obtained numerically by applying equation (1) with the current derived from the streamer modeling.

3. EM Radiation From the Exponentially Growing Sprite Streamers

[5] Stable propagation of streamers requires an applied electric field that is greater than the critical fields $E_{cr}^{\pm}$. The minimum electric field for stable propagation of positive streamers is $E_{cr}^{+} \simeq 4.4\ N/N_0$ kV/cm and that for negative streamers is $E_{cr}^{-} \simeq 12.5\ N/N_0$ kV/cm, where N is the air density at the altitude of interest and $N_0 \simeq 2.688 \times 10^{25}$ m^{-3} is its reference value at ground level [e.g., *Pasko et al.*, 2000]. Streamers propagating in an electric field higher than the critical fields $E_{cr}^{\pm}$ experience an exponential growth

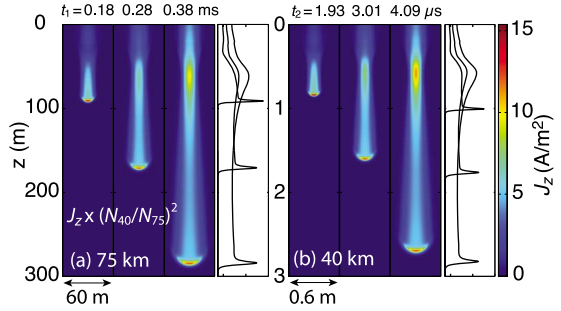

Figure 2. Cross-sectional views of the vertical current densities $J_z(r, z)$ in the body of a sprite streamer initiated from a Gaussian electron density inhomogeneity at (a) 75 km and (b) 40 km in an electric field of $1.0E_k \simeq 28.7\ N/N_0$ kV/cm [*Morrow and Lowke*, 1997]. The one-dimensional curves represent the current density in arbitrary units on the axis of symmetry of the streamers at the same moments of time as that in the 2D plots. Note that $t_2 = t_1\ N_{75}/N_{40}$. The initial inhomogeneity is associated with a peak density of 1.2×10^{11} m^{-3} and a characteristic size of 10 m at 75 km and a peak density of 10^{15} m^{-3} and a characteristic size of 0.1 m at 40 km. The ambient electron density is assumed to be 1.2×10^6 m^{-3} at 75 km (Figure 2a) and 0.6 m^{-3} at 40 km (Figure 2b) [*Qin et al.*, 2012]. Note that the current density $J_z(r, z)$ shown in Figure 2a is $J_z(r, z)$ at 75 km multiplied by $(N_{40}/N_{75})^2$ in order to make direct comparison with $J_z(r, z)$ at 40 km, accounting for quadratic scaling of current density with air density N [*Pasko*, 2006].

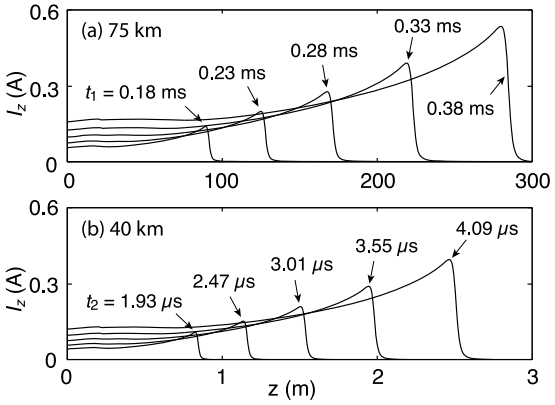

Figure 3. The total vertical current $I(z, t)$ of the streamer at (a) 75 km and (b) 40 km, calculated by integrating the current density $J_z(r, z)$ along the radial direction. Note that $t_2 = t_1\ N_{75}/N_{40}$.

of transverse physical dimension of their heads and propagation speed in time ($\sim\exp(\nu_0 t)$, where ν_0 is the exponential growth rate of streamers) [e.g., *Liu et al.*, 2009; *Celestin and Pasko*, 2011; *Kosar et al.*, 2012; *Qin et al.*, 2012]. *Liu et al.* [2009] and *Kosar et al.* [2012] have calculated that for realistic applied field magnitudes the growth rate ν_0 of streamers at 75 km altitude is on the order of 10^3 s^{-1}, which corresponds to frequencies of $\sim$1 kHz. *Kosar et al.* [2012] have also shown that the exponential growth of streamers propagating under given supercritical fields scales according to the similarity laws for streamer breakdown proposed by *Pasko et al.* [1998] ($\sim 1/N$ at typical sprite altitudes of $\sim$40–90 km where quenching effects of photoionization are negligible [*Liu and Pasko*, 2004]). Note that the air density is $N_{40} \simeq 8.31 \times 10^{22}$ m^{-3} at 40 km and $N_{75} \simeq 8.94 \times 10^{20}$ m^{-3} at 75 km, that leads to a scaling factor of $N_{40}/N_{75} \simeq 93$. Therefore, one can expect that the growth rate of streamers at 40 km altitude is on the order of $10^3 \times N_{40}/N_{75} \simeq 10^5$ s^{-1} corresponding to frequencies of $\sim$100 kHz. It is the main purpose of this section to demonstrate that the exponential growth of the electric current in sprite streamers produces radiation up to $\sim$3 kHz (VLF) at 75 km and up to $\sim$300 kHz (LF) at $\sim$40 km.

[6] Figure 2 shows the vertical current densities $J_z(r, z)$ of two sprite streamers developing at 75 km and 40 km, respectively, with the parameters of the simulation described in the caption. In each case, the current density $J_z(r, z)$ is highly enhanced and rapidly varying in the streamer head that serves as the main radiator, followed by a streamer body with almost constant and relatively weak current density. It is shown that the size of the streamer head R_s (scales as $1/N$) at 75 km is $\sim$100 times larger than that of the streamer head at 40 km, and the current density $J_z(r, z)$ (scales as N^2) at 75 km is $\sim 10^4$ times weaker than that of the streamer at 40 km, which is consistent with the similarity laws (i.e., $N_{40}/N_{75} \simeq 93$).

[7] The vertical current $I_z(z)$ flowing in the streamer body is calculated by integrating the current density $J_z(r, z)$ along the radial direction and shown in Figure 3. Note that the current $I_z(z)$ in the body of the streamer does not depend on air density, since $I_z(z) = J_z(r, z) \times A_s$, where $J_z(r, z)$ scales as N^2 and the area of the streamer cross section $A_s \simeq \pi R_s^2$ scales as N^{-2}. The streamer currents at 75 km and at 40 km

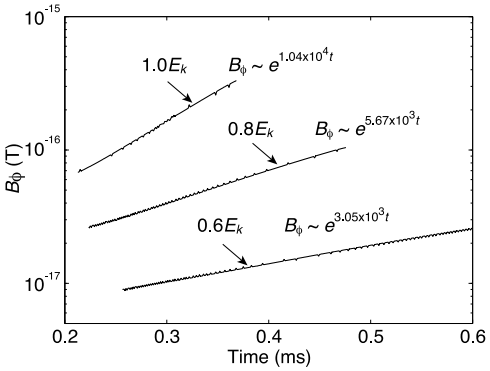

Figure 4. Growth rates of the magnetic field B_ϕ radiated by streamers propagating at 75 km in electric fields of $1.0E_k$, $0.8E_k$, and $0.6E_k$, respectively. The signals are received 600 km away on the ground (see Figure 1).

are therefore comparable. On the other hand, the timescale of the streamer development, which scales as $1/N$, at 40 km is ~93 times shorter than that of the streamer at 75 km (see Figure 3). Therefore, the growth rate ν_0 of the streamer current at 40 km is ~93 times greater than that of the streamer current at 75 km [see also *Kosar et al.*, 2012, Figure 5].

[8] The top curve in Figure 4 shows the growth rate of the magnetic field B_ϕ corresponding to the current variation of a streamer developing at 75 km in an electric field of $1.0E_k$ (see Figure 3a). Note that B_ϕ is obtained by applying equation (1) using current derived from the streamer modeling. Similarly to the growth of radius [*Kosar et al.*, 2012], the growth rate of streamer current is not only a function of altitude (see Figure 3) but also a function of the applied electric field (see Figure 4).

[9] For a magnetic field $B_\phi(t) = \exp(\nu_0 t)$ in arbitrary units that exponentially grows from $t = 0$ to t_0, its spectrum can be calculated analytically from its Fourier transform as follows:

$$B(\omega) = \frac{1}{\sqrt{2\pi}} \int_0^{t_0} e^{\nu_0 t} e^{-j\omega t} \mathrm{d}t = \frac{1}{\sqrt{2\pi}} \frac{e^{(\nu_0 - j\omega)t_0} - 1}{\nu_0 - j\omega} \tag{2}$$

The magnitude of $B(\omega)$ is:

$$|B(\omega)| = \frac{1}{\sqrt{2\pi}} \left(\frac{e^{2\nu_0 t_0} - 2e^{\nu_0 t_0} \cos(\omega t_0) + 1}{\nu_0^2 + \omega^2} \right)^{\frac{1}{2}} \tag{3}$$

where ω is the angular frequency, and for $e^{\nu_0 t_0} \gg 1$, one gets:

$$|B(\omega)| \simeq \frac{1}{\sqrt{2\pi}} \frac{e^{\nu_0 t_0}}{\sqrt{\nu_0^2 + \omega^2}} \tag{4}$$

where $\omega = 2\pi f$ and f is the frequency. Note that the condition $e^{\nu_0 t_0} \gg 1$ can be fulfilled, for example at 75 km, if $t_0 \gtrsim 0.3$ ms since $\nu_0 \simeq 10^4\ \mathrm{s}^{-1}$ (see Figure 4). This spectrum is a square-root Lorentzian density function peaked at $f = 0$ Hz and decreasing rapidly at higher frequency with a half-width of $f_{\mathrm{half}} = \sqrt{3}\nu_0(h, E)/2\pi$. Table 1 lists the f_{half} values for altitudes $h = 75$, 40 km and for field from $E = 0.5$ to $1.0E_k$. Note that the f_{half} values at 75 km in Table 1 are calculated using ν_0 obtained directly from plasma fluid simulations of sprite streamers, whereas these at 40 km are estimated using the values at 75 km and the air density scaling factor $N_{40}/N_{75} \simeq 93$. The f_{half} values at other altitudes h between 40 and 75 km can be estimated using a scaling factor of $\sim\exp\left(\frac{75\ \mathrm{km} - h}{7.72\ \mathrm{km}}\right)$, where 7.72 km is the scale height of the atmospheric density. We test the accuracy of the estimates in Table 1 by calculating f_{half}(40 km, $1.0E_k$) using the streamer current shown in Figure 3b. The result is 271 kHz, and it has a small 1.5% difference from 267 kHz listed in Table 1, which is due to the different ambient electron densities at 75 km and 40 km taken into account in the simulations (see the caption of Figure 2). An important conclusion based on the above results is that sprite streamers propagating at ~40 km altitude would naturally produce LF radiation.

4. EM Radiation From the Periodic Branching of Sprite Streamers

[10] It should be emphasized that the spectrum distribution shown by equation (4) only accounts for the EM radiation from the exponential growth of the current in sprite streamers. Moreover, when the radius of the streamer head becomes several times larger than the photoionization range L_{ph}, the stable growth of sprite streamers is no longer possible, because the density of photoelectrons created ahead of the streamer is insufficient to support the streamer advancement [*Liu and Pasko*, 2004]. These streamers with large heads will split into several small-scale streamers with each head being able to propagate and grow exponentially again [*Liu and Pasko*, 2004]. Note that the photoionization range L_{ph}, that is determined by the absorption length of UV photons by oxygen molecules, is inversely proportional to the air density N and therefore decreases exponentially with decreasing altitude. This streamer branching phenomenon has been commonly observed in high-speed video observations of sprites [e.g., *Cummer et al.*, 2006; *McHarg et al.*, 2010], and it is also clearly shown in these videos that sprite streamers branch more frequently when propagating toward lower altitudes where the photoionization range L_{ph} is shorter.

[11] It is reasonable to assume that the vertical current $I_z(z)$, that increases exponentially before the sprite streamers branch (see Figure 3), may experience a sudden decrease during the extremely rapid process of branching, since right after branching most of the small-scale streamers do not propagate vertically (see the streamer branching process shown in *McHarg et al.* [2010]). After this sudden decrease, the vertical current $I_z(z)$ starts another round of exponential growth before the sprite streamers branch again. When propagating downwards, the branching of sprite streamers occurs more frequently and introduce periodicity in the variation of vertical streamer current that may lead to narrow-band enhancements in the spectrum of sprite radiation.

[12] The time interval between two successive streamer branching (i.e., the period T_{b} of the vertical current variation that determines the peak frequencies in the spectrum of sprite radiation) is a function of air density N, and its order of

Table 1. Half-Width of the Spectrum of B_ϕ (kHz) as a Function of Altitude and Applied Electric Field

	$1.0E_k$	$0.9E_k$	$0.8E_k$	$0.7E_k$	$0.6E_k$	$0.5E_k$
75 km	2.87	2.09	1.56	1.17	0.84	0.59
40 km	267	194	145	109	78	55

magnitude can be estimated using the following two different approaches leading to similar results.

[13] The first approach is based on the theoretical work of *Liu and Pasko* [2004] in which the photoionization range L_{ph} is stated to be $(\chi_{min} p_{O2})^{-1}$ and $L_{ph} \simeq 0.2$ cm at ground pressure in air, where χ_{min} and p_{O2} are the absorption coefficient and the partial pressure of molecular oxygen, respectively. *Celestin and Pasko* [2011] estimated that the value of the branching radius R_b is ~0.5 cm at ground pressure and then found the corresponding time of streamer branching $T_{b0} \simeq 11.2$ ns and the corresponding streamer length $L(t_b) = 7$ cm. Using the air density scaling factors, while neglecting the non-similarity of photoionization, we find that at 40 km $T_{b40} \simeq 3.62$ μs corresponding to frequencies of ~276 kHz, and at 75 km $T_{b75} \simeq 0.34$ ms corresponding to frequencies of ~2.97 kHz.

[14] The second approach is based on the experimental work of *McHarg et al.* [2010] in which successive branching of sprite streamer propagating at ~75 km has been clearly documented with sub-millisecond time resolution. The example used in this estimate is the one presented in *McHarg et al.* [2010, Figure 2], which shows that a sprite streamer split at ~76 km into five small streamers that propagated down to ~70 km altitude where they split again into smaller streamers. Assuming that the streamer velocity was 1.8×10^7 m/s [*McHarg et al.*, 2010], the time interval between successive branching at ~75 km is 0.33 ms corresponding to frequencies of ~3.00 kHz. Using the air density scaling factor of ~93, at 40 km the time interval is ~3.58 μs corresponding to frequencies of ~279 kHz.

[15] The results obtained from the above two different approaches agree well. However, we emphasize that existing high-speed observations are not yet able to resolve the branching dynamics at low altitudes and the actual frequencies of the radiation from the periodic branching of sprite streamers at 40 km may be lower than the above estimates because the reduced electric field at 40 km produced by the lightning discharge is small, which leads to slow growth of sprite streamers. Nevertheless, the above estimates, along with the calculations in Section 3, predict that in the case of +CGs associated with large charge moment changes, sprite streamers that are able to propagate down to ~40 km altitude can radiate electromagnetic field with frequencies in the LF range (30–300 kHz).

5. Observability of Sprite Radiation

[16] We note that stable propagation of streamers requires the lightning-induced quasi-static electric field to be larger than the critical field $E_{cr}^{\pm}$ as discussed in Section 3. Therefore, for streamers to propagate down to ~40 km, a large charge moment change of ~1000 C km is necessary. Besides, a large charge moment change that leads to a large streamer initiation region is also more likely to produce a large constellation of sprites (e.g., jellyfish sprites) [*Qin et al.*, 2011, 2012], which may be one necessary condition for sprite radiation to be detectable (see figures in *Cummer et al.* [1998]). Note that when measured several hundred kilometers away from the parent lightning discharge, the typical magnitude of the magnetic field radiated by sprite current is on the order of 10^{-9} T [e.g., *Cummer et al.*, 1998; *Cummer*, 2003]. The number of streamers required to produce this amount of radiation can be estimated using Figures 3a and 4. In Figure 3a, the length of the streamer grows exponentially in time, and using extrapolation (see *Liu et al.* [2009] and discussion therein) it is found that it takes ~1 ms for this streamer to become 6 km long. In ~1 ms, the magnetic field shown by the top curve in Figure 4 grows up to $\sim 1.2 \times 10^{-12}$ T. Having assumed that this is the largest magnitude of the magnetic field radiated by an individual streamer, since branching occurs after streamer propagates ~6 km at 75 km altitude [*McHarg et al.*, 2010], it requires ~1000 individual streamers to produce the magnitude of the sprite radiation measured by *Cummer et al.* [1998] and *Cummer* [2003].

6. Conclusions

[17] In the present study, we demonstrate that the spectral content of the electromagnetic radiation from sprite streamers is highly dependent on the air density N, i.e., sprite streamers at lower altitudes with higher air density N produce a higher frequency radiation. We calculate that the exponential growth of the streamer current with a rate ν_0 of $\sim 10^3$ s^{-1} at ~75 km produces radiation with frequencies up to ~3 kHz, whereas at ~40 km with a rate ν_0 of $\sim 10^5$ s^{-1} it produces a radiation with frequencies up to ~300 kHz. The ideal spectrum due to this exponential growth is a "square-root" Lorentzian density function peaked at $f = 0$ Hz and decreasing rapidly at higher frequency with a half-width of $f_{half} = \sqrt{3}\nu_0/2\pi$, where ν_0 scales as the air density N and is a function of the lightning-induced electric field E. We also conjecture that the streamer branching process may introduce periodicity in the streamer current variation thus would lead to sprite radiation enhanced in the ELF (10 Hz–3 kHz) range for sources at 75 km and enhanced in the LF (30–300 kHz) range for sources at 40 km. The above-discussed frequency variation at different altitudes obeys the similarity laws for streamer breakdown proposed by *Pasko et al.* [1998], and therefore frequencies of streamer radiation at other altitudes can be estimated using linear scaling with air density N. Frequencies in the LF range associated with sprites have already been detected and interpreted as produced by relativistic electron beams [*Fullekrug et al.*, 2010, 2011]. The present study shows that sprite streamers could be responsible for at least part of this radiation. We further note that the charge moment change of the sprite-causative lightning discharge that determines the altitude range of the streamer propagation determines the spectrum of the sprite radiation. A lightning discharge associated with a large charge moment change not only enable streamer propagation down to low altitudes but also would be more likely to produce a large constellation of sprites (e.g., jellyfish sprites). In turn, this would likely produce electromagnetic radiation with a detectable magnitude.

[18] **Acknowledgments.** This research was supported by the NSF grant AGS-0734083 and DARPA NIMBUS grant HR0011-101-0059/10-DARPA-1092 to the Pennsylvania State University.

[19] The Editor thanks two anonymous reviewers for their assistance in evaluating this paper.

References

Bourdon, A., V. P. Pasko, N. Y. Liu, S. Celestin, P. Segur, and E. Marode (2007), Efficient models for photoionization produced by non-thermal gas discharges in air based on radiative transfer and the Helmholtz equations, *Plasma Sources Sci. Technol.*, *16*, 656–678.

Celestin, S., and V. P. Pasko (2011), Energy and fluxes of thermal runaway electrons produced by exponential growth of streamers during the stepping of lightning leaders and in transient luminous events, *J. Geophys. Res.*, *116*, A03315, doi:10.1029/2010JA016260.

Cummer, S. A. (2003), Current moment in sprite-producing lightning, *J. Atmos. Sol. Terr. Phys.*, *65*, 499–508.

Cummer, S. A., U. S. Inan, T. F. Bell, and C. P. Barrington-Leigh (1998), ELF radiation produced by electrical currents in sprites, *Geophys. Res. Lett.*, *25*, 1281–1284.

Cummer, S. A., N. C. Jaugey, J. B. Li, W. A. Lyons, T. E. Nelson, and E. A. Gerken (2006), Submillisecond imaging of sprite development and structure, *Geophys. Res. Lett.*, *33*, L04104, doi:10.1029/2005GL024969.

Fullekrug, M., D. R. Moudry, G. Dawes, and D. D. Sentman (2001), Mesospheric sprite current triangulation, *J. Geophys. Res.*, *106*, 20,189–20,194.

Fullekrug, M., R. A. Roussel-Dupre, E. M. D. Symbalisty, O. Chanrion, A. Odzimek, O. V. der Velde, and T. Neubert (2010), Relativistic runaway breakdown in low-frequency radio, *J. Geophys. Res.*, *115*, A00E09, doi:10.1029/2009JA014468.

Fullekrug, M., et al. (2011), Relativistic electron beams above thunderclouds, *Atmos. Chem. Phys.*, *11*(15), 7747–7754, doi:10.5194/acp-11-7747-2011.

Kosar, B. C., N. Liu, and H. K. Rassoul (2012), Luminosity and propagation characteristics of sprite streamers initiated from small ionospheric disturbances at subbreakdown conditions, *J. Geophys. Res.*, *117*, A08328, doi:10.1029/2012JA017632.

Liu, N. Y., and V. P. Pasko (2004), Effects of photoionization on propagation and branching of positive and negative streamers in sprites, *J. Geophys. Res.*, *109*, A04301, doi:10.1029/2003JA010064.

Liu, N. Y., V. P. Pasko, K. Adams, H. C. Stenbaek-Nielsen, and M. G. McHarg (2009), Comparison of acceleration, expansion, and brightness of sprite streamers obtained from modeling and high-speed video observations, *J. Geophys. Res.*, *114*, A00E03, doi:10.1029/2008JA013720.

McHarg, M. G., H. C. Stenbaek-Nielsen, T. Kanmae, and R. K. Haaland (2010), Streamer tip splitting in sprites, *J. Geophys. Res.*, *115*, A00E53, doi:10.1029/2009JA014850.

Morrow, R., and J. J. Lowke (1997), Streamer propagation in air, *J. Phys. D Appl. Phys.*, *30*, 614–627.

Pasko, V. P. (2006), Theoretical modeling of sprites and jets, in *Sprites, Elves and Intense Lightning Discharges*, *NATO Sci. Ser., Ser. 2*, vol. 225, edited by M. Füllekrug, E. A. Mareev, and M. J. Rycroft, pp. 253–311, Springer, Heidleberg, Germany.

Pasko, V. P., U. S. Inan, and T. F. Bell (1998), Spatial structure of sprites, *Geophys. Res. Lett.*, *25*, 2123–2126.

Pasko, V. P., U. S. Inan, and T. F. Bell (2000), Fractal structure of sprites, *Geophys. Res. Lett.*, *27*(4), 497–500, doi:10.1029/1999GL010749.

Qin, J., S. Celestin, and V. P. Pasko (2011), On the inception of streamers from sprite halo events produced by lightning discharges with positive and negative polarity, *J. Geophys. Res.*, *116*, A06305, doi:10.1029/2010JA016366.

Qin, J., S. Celestin, and V. P. Pasko (2012), Formation of single and double-headed streamers in sprite-halo events, *Geophys. Res. Lett.*, *39*, L05810, doi:10.1029/2012GL051088.

Stenbaek-Nielsen, H. C., and M. G. McHarg (2008), High time-resolution sprite imaging: Observations and implications, *J. Phys. D Appl. Phys.*, *41*, 234009.

Uman, M. A., D. K. McLain, and E. P. Krider (1975), The electromagnetic radiation from a finite antenna, *Am. J. Phys.*, *43*(1), 33–38, doi:10.1119/1.10027.